

# Poly(ether urethane)/Poly(ethyl methacrylate) IPNs with High Damping Characteristics: The Influence of the Crosslink Density in Both Networks

DOUGLAS J. HOURSTON\* and FRANZ-ULRICH SCHÄFER

Institute of Polymer Technology and Materials Engineering, Loughborough University, Loughborough LE11 3TU, United Kingdom

## SYNOPSIS

Interpenetrating polymer networks (IPNs) with a controlled degree of microphase separation were synthesized from a poly(ether urethane) (PUR) and poly(ethyl methacrylate) (PEMA). The influence of the crosslink density of both networks was investigated in the 70 : 30 PUR/PEMA IPN. The extent of damping was evaluated by dynamic mechanical thermal analysis. Mechanical properties were studied using tensile testing and hardness measurements. Control of crosslinking was successful in tailoring the damping profile. Higher crosslinking in the first-formed network (polyurethane) seemed to increase slightly the area under the linear loss modulus curve, LA, whereas no influence was obvious when changing the crosslink density in the second network. TGA studies revealed improved thermal properties for the IPNs with a higher crosslink density in the PUR network. TEM micrographs confirmed a finer morphology for the materials with a higher crosslink density in the PUR, whereas increasing the crosslink density in the PEMA network resulted in a decrease of phase mixing. © 1996 John Wiley & Sons, Inc.

## INTRODUCTION

Interpenetrating polymer networks (IPNs) are an intimate blend of two network polymers with very special properties.<sup>1,2</sup> These special properties are brought about by permanent interlocking of chains through chemical crosslinks.<sup>3</sup> Thus, in IPNs crosslinking can be used as a means to restrict the phase domain size and often a very fine phase morphology is obtained. It has been found<sup>4</sup> that crosslinking can influence reaction kinetics and phase continuity. The network that forms first<sup>5</sup> is likely to represent the continuous phase, and, thus, determines the IPN properties. Transmission electron microscopy studies<sup>6</sup> revealed that high crosslinking of the first-formed network restricts the phase domain size for the second polymer. As a consequence, the crosslink density in the polymer networks greatly influences

the mechanical properties and the damping properties.

In the present study, the influence of the crosslink density in both networks in a poly(ether urethane) (PUR)/poly(ethyl methacrylate) (PEMA) IPN was investigated. Few studies<sup>7-9</sup> have been conducted on PUR/PEMA IPNs. In one such study,<sup>7</sup> the damping ability of 70 : 30 PUR/(meth)acrylates was compared. It was found that PUR/PEMA and PUR/PEA IPNs had larger loss areas than their methyl counterparts (PUR/PMMA and PUR/PMA). This was explained<sup>7</sup> in terms of the pendent ethyl side chain imparting more damping than the methyl chain. In a recent study,<sup>8</sup> the phase continuity of the full composition range of PUR/PEMA IPNs was studied relating experimental data to composition-modulus theories. The 70 : 30 PUR/PEMA composition was found to exhibit a number of synergistic properties. Stress-strain measurements resulted in maxima for the elongation at break and the toughness index.<sup>8</sup> An investigation<sup>9</sup> of the damping ability of these IPNs by dynamic mechanical thermal analysis revealed a very broad, almost rectangular, tran-

\* To whom correspondence should be addressed.

sition range with high values for the area under the linear loss factor curve, TA. The PUR and the PEMA loss factor peaks were of equal height, which has been found<sup>3,10</sup> to be an indication of dual phase continuity.

Consequently, the 70 : 30 PUR/PEMA IPN composition was chosen for this crosslinking study. The influence of crosslinking on the morphology, the thermal, and the mechanical properties was determined using transmission electron microscopy, thermogravimetric analysis, and stress-strain and hardness measurements. Dynamic mechanical thermal analysis was conducted in order to determine the inherent damping of the materials. The latter was characterized in terms of the range over which  $\tan \delta > 0.3$  and the areas under the linear loss factor (TA) and loss modulus (LA) curves.

## EXPERIMENTAL

### Materials

Poly(oxypropylene) glycol of a molar mass of 1025 (PPG1025, supplied by BDH) was used as the PUR soft segment. The hard segment was formed from the 1,1,3,3,-tetramethylxylene diisocyanate (m-TMXDI, kindly donated by Cytec), and the crosslinker was trimethylol propane (TMP, supplied by Aldrich). Stannous octoate (SnOc, supplied by Aldrich) was used as the PUR catalyst. Ethyl methacrylate monomer (EMA, supplied by Aldrich) was crosslinked with tetraethylglycol dimethacrylate (TEGDM, supplied by BDH) and initiated with azoisobutyronitrile (AIBN, supplied by BDH).

### IPN Preparation

The IPN preparation has been described in an earlier publication.<sup>4</sup> In brief, the TMP was dissolved in the PPG1025 at 60°C. At room temperature, the polymer component mixture including EMA, TEGDM and the dissolved AIBN were added. Upon addition of the SnOc and the TMXDI, the components were stirred under a nitrogen blanket for 5 min. After degassing for 1 min at high vacuum, the mixture was molded in an O-ring mold. Curing was conducted in three cycles of 24 h at 60, 80, and 90°C.

### Dynamic Mechanical Thermal Analysis (DMTA)

DMTA measurements were conducted with a Polymer Laboratories MKII Dynamic Mechanical Analyser in the bending mode (single cantilever). The

temperature program was run from -60 to 200°C using a heating ramp of 3°C/min at a fixed frequency of 10 Hz. The applied strain setting was  $\times 4$ .

### Tensile Testing

Stress-strain analyses were conducted using a Lloyd 1 2000R instrument equipped with a 500 N load cell. A crosshead speed of 50 mm/min was chosen. Small size dumb-bells with a gauge length of 30 mm were used in this study. Tests were conducted at 23°C  $\pm$  1°C and the values quoted are an average of 4-5 samples.

### Hardness Measurements

Shore A hardness was determined using a Zwick model 3114 durometer. The testing was conducted at room temperature (23  $\pm$  1°C). Hardness values quoted are from an average of eight readings taken at random over the entire specimen surface.

### Thermogravimetric Analysis (TGA)

4-6 mg samples were analyzed in an air atmosphere using a TG 760 Series Rheometric Scientific instrument. The heating ramp used was 10°/min from room temperature to 700°C.

### TEM Micrographs

The elastomeric samples were embedded in epoxy resin and ultramicrotomed into 100 nm thick sections. Staining was conducted for 48 h in a 2% osmium tetroxide solution. The electron micrographs were taken with a Jeol Jem 100 CX instrument using an accelerating voltage of 60 kV.

## RESULTS AND DISCUSSION

The chemical crosslinks give the IPNs their special properties. However, at the same time, the thermoset character make IPNs very difficult to characterize.<sup>11</sup> Characterization techniques such as equilibrium swelling are difficult to evaluate, since contributions from each network cannot be subdivided into the individual components. Consequently, mainly the theoretical average molecular weight between crosslinks,  $M_{c,t}$ , was calculated in this study. For the crosslink densities synthesized in the IPNs, the  $M_{c,t}$  of the homopolymers are presented in Table I. The crosslink density of the PUR network was varied by altering the diol/triol ratio.  $M_{c,t}$  was calculated using

Table I Crosslink Densities of Both Networks for the 70 : 30 PUR/PEMA Composition

Crosslinking Homopolymers	Average $M_c$			
	$T_g$ [tan $\delta$ , °C]	Theoretical	Swelling	Nielson Equ.
Polyurethane				
diol/triol 1 : 1	30	1180	3200	940
2 : 1	4	2030	4400	2440
3 : 1	-5	2870	6100	5200
7 : 1	-9	6260	10000	13000
1 : 0	-12	—	—	—
Polyethyl methacrylate				
crosslinker 10%		680	a	a
5%	105	1250	—	1900
2.5%		2390	a	a
1%		5810	a	a
0%		—	—	—

<sup>a</sup> Material not synthesized.

the following equation, derived from the assumptions that a stoichiometric equivalent ratio of NCO to OH functionalities was present, no secondary PUR reactions, such as the formation of allophanate crosslinks, and no autoaddition of diisocyanates to form dimers and trimers occurred and that the formation of this ideal network went to completion.

$$M_{c,t} = \frac{dM_D + tM_T + (2d + 3t)M_I/2}{3t/2} \quad (1)$$

Here  $d$  and  $t$  are the moles of diol and triol,  $M_D$ ,  $M_T$ , and  $M_I$  represent the molar mass of the diol, triol, and diisocyanate, respectively. The ratio of the crosslinking agent, TEGDM, for the PEMA network was also altered.  $M_{c,t}$  was calculated using a modification of a previously reported equation.<sup>12</sup>

$$M_{c,t} = \frac{X_M M_M + X_X M_X}{2X_X} \quad (2)$$

$X_M$  and  $X_X$  are the mole fractions and  $M_M$  and  $M_X$  are the molar masses of the monomer and crosslinker, respectively. Because of the high TEGDM molar mass of 330 g/mol, this was taken into account by the second component in the sum.

For both homonetworks, these theoretical  $M_c$  values were compared with experimental values obtained from equilibrium swelling and from an empirical equation developed by Nielson.<sup>13</sup> In order to be able to apply Nielson's equation, the linear PUR and a series of polyurethane homonetworks were synthesized at the diol/triol ratios of the IPNs. The

dynamic mechanical data for these materials are shown in Figure 1.

From these data, the approximate value of  $M_c$  can be determined using the difference between the  $T_g$  of the linear polymer and the crosslinked equivalents. The following empirical equation has been suggested<sup>13</sup> to give approximate  $M_c$ .

$$T_g - T_{g_0} = \frac{3.9 \cdot 10^4}{M_c} \quad (3)$$

$T_g$  is the glass transition temperature of the crosslinked polymer and  $T_{g_0}$  the glass transition temperature of the linear equivalent. Using this equation, approximate  $M_c$  values for the PUR homonetworks were obtained (Table I). Also,  $M_c$  for the PEMA homonetwork crosslinked with 5% TEGDM was determined. Comparing the theoretical  $M_c$  values with the values obtained by the Nielson equation, a similar trend was noticed. However, whereas the  $M_c$  values for the more crosslinked materials were relatively close, the Nielson equation predicted a much lower crosslink density at low triol levels. For the 5% crosslinked PEMA network, a much lower crosslink density than the theoretical value was found.

The average molecular weight between crosslinks of these homopolymers was also determined via swelling studies using the Flory-Rehner<sup>14,15</sup> equation.

$$\nu_e = -\frac{1}{V_s} \left[ \frac{\ln(1 - \nu_r) + \nu_r + \chi \nu_r^2}{\nu_r^{1/3} - 2\nu_r/F} \right] \quad (4)$$

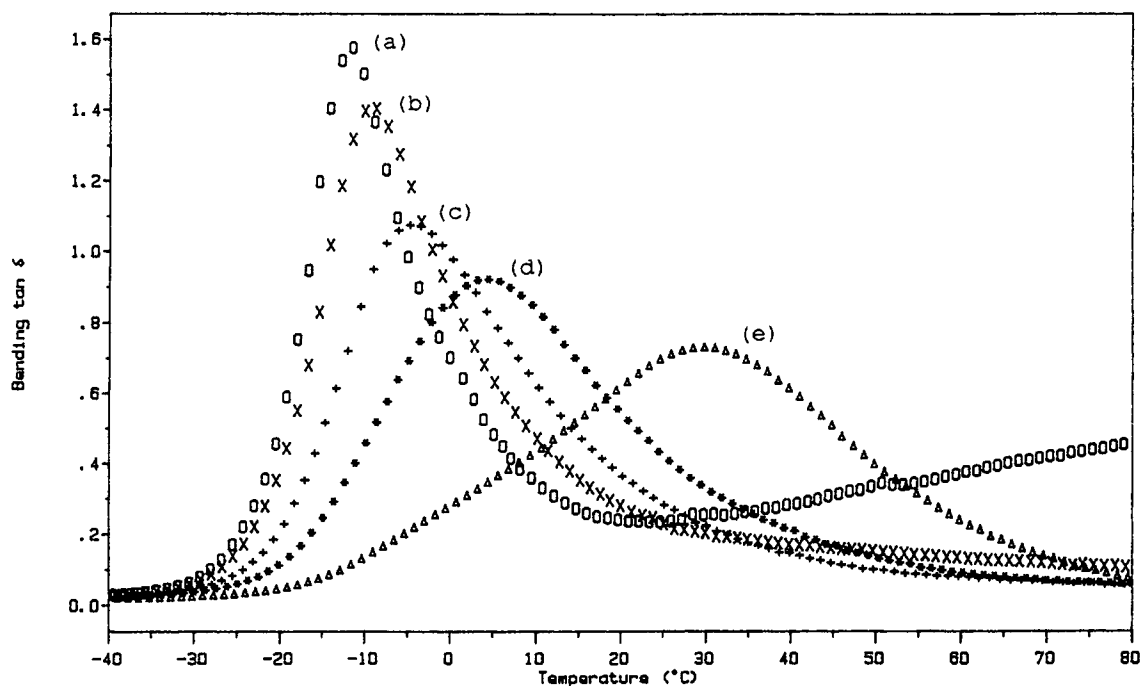


**Figure 1** Loss factor versus temperature data for PUR homonetworks of different cross-linking levels. (a) Diol/triol 1 : 0, (b) 7 : 1, (c) 3 : 1, (d) 2 : 1 and (e) 1 : 1.

$\nu_e$  is the number of polymer chains per unit volume,  $V_s$  is the molar volume of swelling agent,  $\nu_r$  is the volume fraction of polymer in the swollen gel,  $\chi$  is the polymer-solvent interaction parameter, and  $F$  the functionality of the system. The polymer-solvent interaction parameter was determined using the semiempirical Bristow and Watson<sup>16</sup> equation,  $\chi = \beta + (V_s/RT)(\delta_s - \delta_p)^2$ , where  $\beta$  is the lattice constant (usually about 0.34), and  $\delta$  the solubility parameter of the solvent and the polymer.  $\nu_e$  and  $M_c$  are related by the polymer density  $\rho$ .

$$\nu_e = \frac{\rho}{M_c} \quad (5)$$

For the PUR networks, all average  $M_c$  values determined by swelling studies were higher than the theoretical ones. Furthermore, the  $M_c$  values at low triol content were closer to the theoretical values (higher by a factor of 1.6) than the ones at high triol content (higher by a factor of 2.7). This can be explained by the fact that at a high crosslink density there were more unreacted functional groups left in the material. This occurs because of the decrease in chain mobility in the curing network.

In this study of the influence of the crosslink density, only the 70 : 30 PUR/PEMA composition was investigated. However, for a better general un-

derstanding, the loss factor data for the PUR homonetwork, the 70 : 30 PUR/PEMA IPN and the PEMA homonetwork are shown in Figure 2.

The PUR network was crosslinked with a diol/triol ratio of 3 : 1 while 5% TEGDM crosslinker was incorporated into the PEMA network. A broad, almost rectangular, transition spanning a wide temperature range was obtained for the 70 : 30 PUR/PEMA IPN. This IPN was taken as the base material and the crosslink densities in both networks were varied. Figure 3 shows the loss factor versus temperature data for various crosslink levels of the polyurethane network in the 70 : 30 PUR/PEMA IPN (the PEMA crosslink level was kept constant at 5% TEGDM).

The loss factor data showed, as expected, that with increasing triol content, the PUR transition moved to increasingly higher temperatures. The glass transition temperatures ( $T_g$ ) for these materials taken at the loss factor maximum (10 Hz) are shown in Table II.

The semi-1 IPN, which was synthesized by leaving out the PUR triol component, had the lowest  $T_g$  with  $-16^\circ\text{C}$ . At  $60^\circ\text{C}$ , this material became too soft for measurement and the loss factor values went off scale. With increasing triol content in the PUR, the  $T_g$  shifted to higher temperatures. The highest  $T_g$  of  $54^\circ\text{C}$  resulted with the highest diol/triol ratio of

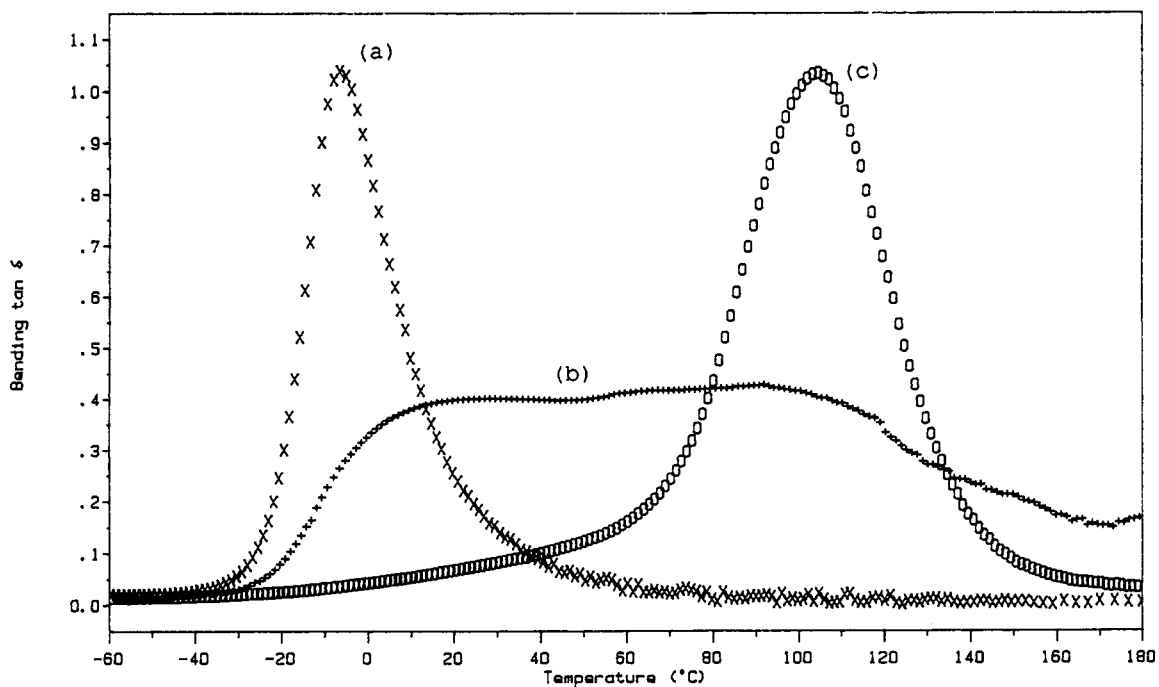


**Figure 2** Comparison of the loss factor versus temperature data between (a) the PUR homonetwork (diol/triol 3 : 1), (b) the 70 : 30 PUR (diol/triol 3 : 1)/PEMA (5% TEGDM) IPN and (c) the PEMA (5% TEGDM) homonetwork.

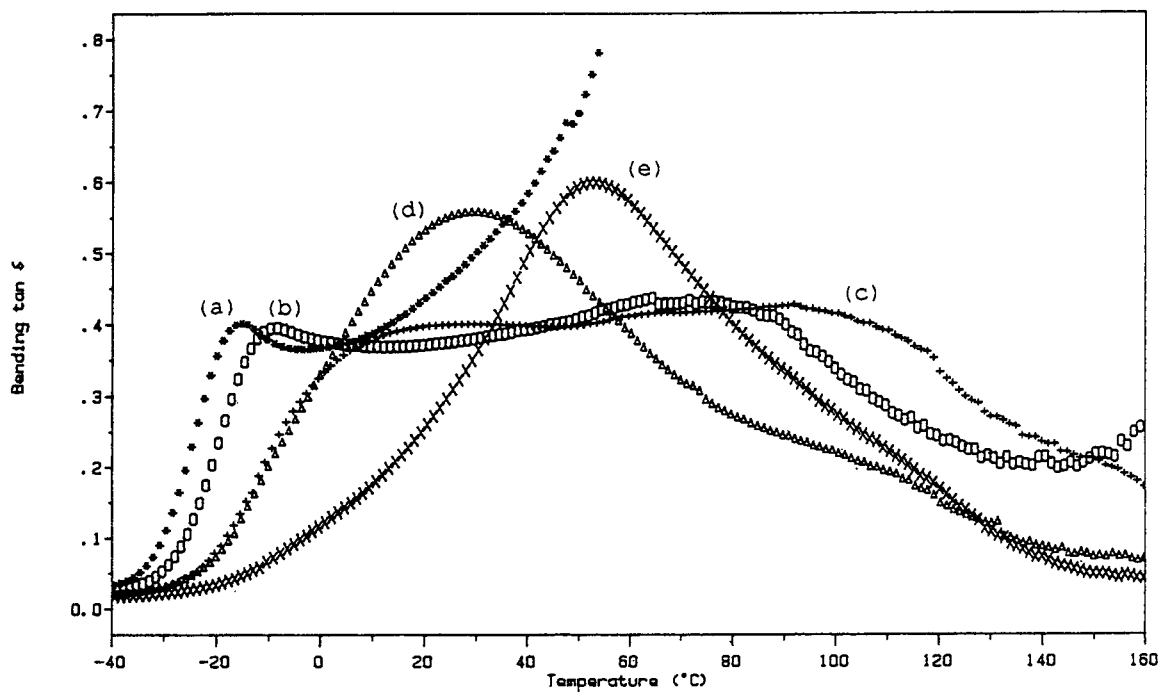


**Figure 3** Loss factor versus temperature data for the 70 : 30 PUR/PEMA (5% TEGDM) IPN with different PUR network crosslinking levels. (a) Diol/triol 1 : 0, (b) 7 : 1, (c) 3 : 1, (d) 2 : 1 and (e) 1 : 1.

**Table II** Dynamic Mechanical Properties (10 Hz) of the 70 : 30 PUR/PEMA IPN (and the Homonetworks) as a Function of Crosslink Density

Crosslinking IPN	$T_g$ [tan $\delta$ , °C]		an $\delta$ Maximum		$\frac{1}{2}$ Peak Width (°C)
	PUR	PEMA	PUR	PEMA	
1 : 1/5%	54	<sup>a</sup>	0.60	—	72
2 : 1/5%	29	<sup>a</sup>	0.55	—	82
3 : 1/10%	18	95	0.47	0.26	118
3 : 1/5%	18	87	0.40	0.42	156
3 : 1/2.5%	20	75	0.43	0.42	131
3 : 1/1%	45	<sup>a</sup>	0.50	—	111
3 : 1/0%	29	<sup>a</sup>	0.60	—	84
7 : 1/5%	-9	75	0.39	0.43	149
1 : 0/5%	-16	<sup>b</sup>	0.40	<sup>b</sup>	<sup>b</sup>
1 : 0/0%	-16	36	0.30	0.75	(97) <sup>c</sup>
100 PUR (3 : 1) <sup>c</sup>	-5	—	1.08	—	28
100 PEMA (5%) <sup>c</sup>	—	105	—	1.04	42

<sup>a</sup> No glass transition temperature for the second component could be determined.

<sup>b</sup> Material became too soft for measurement.

<sup>c</sup> For values in brackets substantial curve extrapolation had to be conducted.

1 : 1. Comparing the loss factor data of the PUR homonetworks (Fig. 1 and Table I) with the respective ones of the IPNs (Figure 2 and Table II) with similar PUR crosslink density showed a similar trend. However, contrary to the IPNs, the loss factor peak height increased with increased PUR crosslink density in the IPN, whereas the values for the tan  $\delta$  were higher at lower crosslink level for the pure PUR networks. Further, two peculiarities for the IPN loss factor peak locations were noted. The  $T_g$  of the linear PUR homonetwork was higher (-12°C) than that of the IPN containing the linear PUR (-16°C). This can be explained by a plasticization effect<sup>17,18</sup> of PEMA chains being dissolved in PUR-rich domains, and, thus, decreasing the PUR-PUR interactions. More likely perhaps is that the molecular weight of the PUR was somewhat lowered in the IPN because of an incomplete reaction caused by a dilution effect of the PEMA. At high crosslinking, for example, at a diol/triol ratio of 1 : 1, the opposite effect was observed. The  $T_g$  of the PUR homonetwork (30°C) was clearly lower than that of the IPN (54°C). For the IPN, though, only one  $T_g$  was observed. Consequently, the intimate mixing of the PUR and the PEMA resulted in only one transition, which explained the transition shift to the higher temperature, proving that an increase in crosslink density in the PUR network improved polymer mixing.

Besides the loss factor peak location, the loss factor maximum and loss factor half-peak width were

also recorded for the IPNs (Table II). The loss factor peak heights are commonly used to obtain information about the continuous phase,<sup>3</sup> with the material exhibiting the higher loss factor peak usually representing the continuous phase. The loss factor half-peak width<sup>19</sup> has been used as an indication of the miscibility of IPNs, with a narrower peak indicating better miscibility. The loss factor peak height increased with increasing crosslinking in the PUR. This was mainly because of the fact that higher crosslinking caused better mixing of the IPN components, which resulted in a combination of the two transition peaks. At diol/triol ratios of 3 : 1 and 7 : 1, the loss factor peaks of the PUR and the PEMA were roughly of equal height, which suggested dual-phase continuity in these IPNs. As for the loss factor half-peak widths, they were generally found to decrease with higher crosslinking in the PUR component. This was a consequence of the PUR transition shifting to higher temperatures, combined with some forced mixing of the PUR and PEMA. The latter was obvious in the PEMA shoulder becoming less noticeable and being more and more dominated by the PUR transition. The linear loss modulus versus temperature data for three IPN materials from this series are shown in Figure 4.

It was noted that increasing the crosslinking in the IPNs resulted in a broader, yet lower, linear loss modulus versus temperature curve. Also, the maximum shifted to higher temperatures.

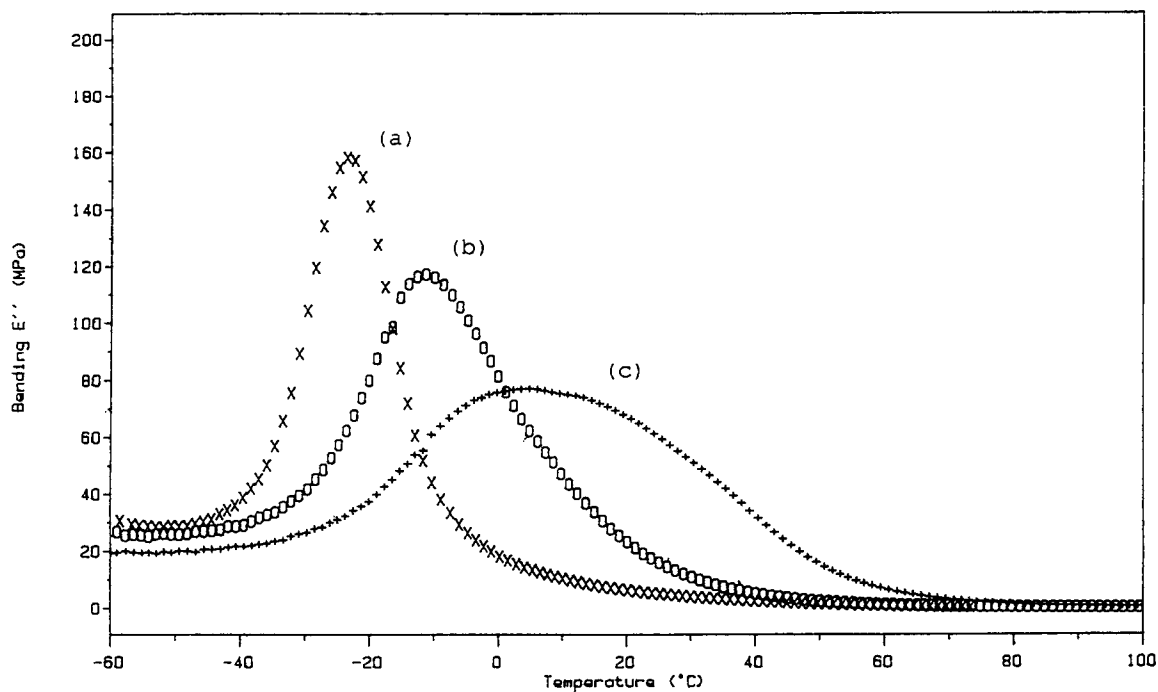


**Figure 4** Loss modulus versus temperature data for the 70 : 30 PUR/PEMA (5% TEGDM) composition with different PUR network crosslinking levels. (a) Diol/triol 1 : 0, (b) 2 : 1 and (c) 1 : 1.

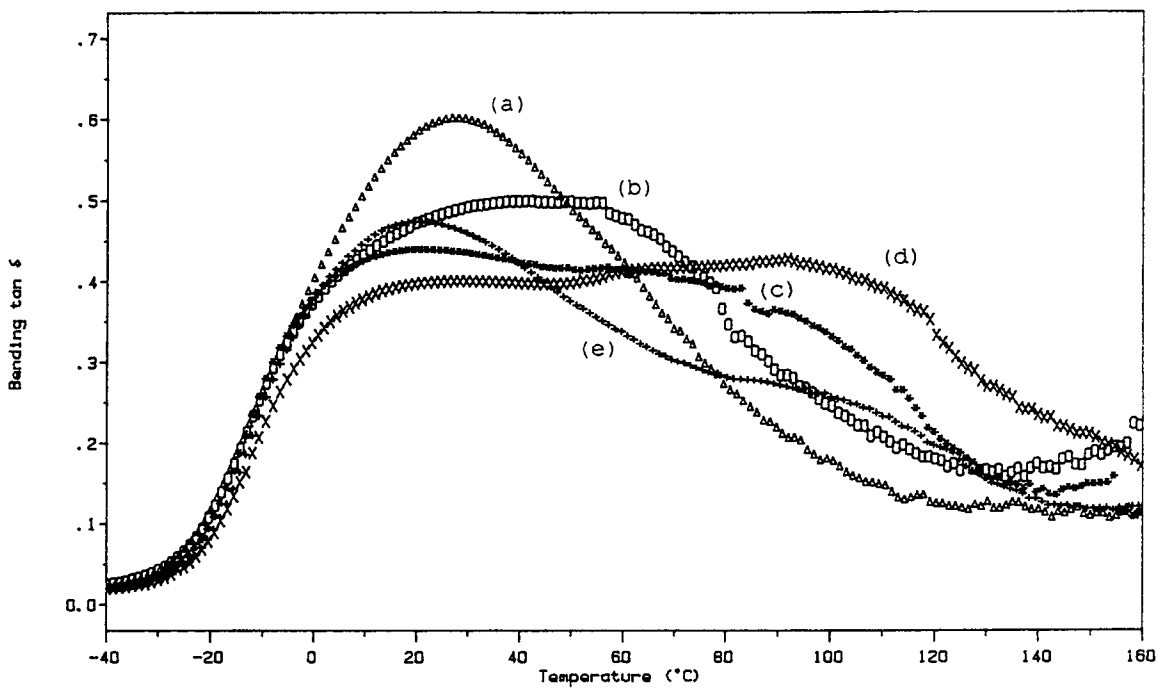


**Figure 5** Loss factor versus temperature data for the 70 : 30 PUR (diol/triol 3 : 1)/PEMA IPN with different PEMA network crosslinking levels. (a) 0% TEGDM, (b) 1%, (c) 2.5%, (d) 5% and (e) 10%.

Besides the crosslinking density in the PUR, the crosslink density in the PEMA component was also varied while keeping the diol/triol ratio fixed at 3 : 1. The loss factor versus temperature data for the different PEMA crosslink densities are shown in Figure 5.

Increasing the crosslinker level moved part of the IPN transition to higher temperatures. The transition was found to split into two parts, with the PUR part shifting to slightly lower temperatures, whereas the PEMA strongly shifted to higher temperatures (Table II). Thus, as opposed to higher crosslinking in the PUR, higher crosslinking in the PEMA generally resulted in a broadening of the IPN transition peak. The semi-2 IPN with 0% TEGDM crosslinker exhibited the narrowest loss factor half-peak width with an 84°C value (Table II). This suggested that the best mixing occurred with this material. With increasing amount of crosslinker, the transition breadth increased and the PEMA part moved to higher temperatures. At 1% incorporation level, a single, clearly broader transition peak was, however, still obtained, which manifested itself in a greater value for the half-peak width (111°C).

With 2.5% TEGDM, a split of the transition peak occurred, with part of it moving to lower temperatures (the PUR transition) and the appearance of a very significant shoulder at the high temperature side. The material with the broadest transition with a half-peak width of 156°C was obtained with 5% TEGDM crosslinking. Further increasing the crosslinking to 10% TEGDM led to a significant decrease of the transition height for the PEMA because of reduced chain segment mobility.

The differences observed between increasing the crosslink density in the PUR and in the PEMA component might be explained by the following points. Increasing the PEMA crosslinking shifted the transition to higher temperatures, thus away from the PUR transition, whereas higher crosslinking in the PUR shifted the transition toward the PEMA transition. Higher crosslinking in the first-formed PUR network increased phase mixing by restricting the domain size of the PEMA network. Higher crosslinking of the PEMA network had little or no influence on the already formed PUR network and decompatibilized the IPN by decreasing the PEMA chain segment mobility.

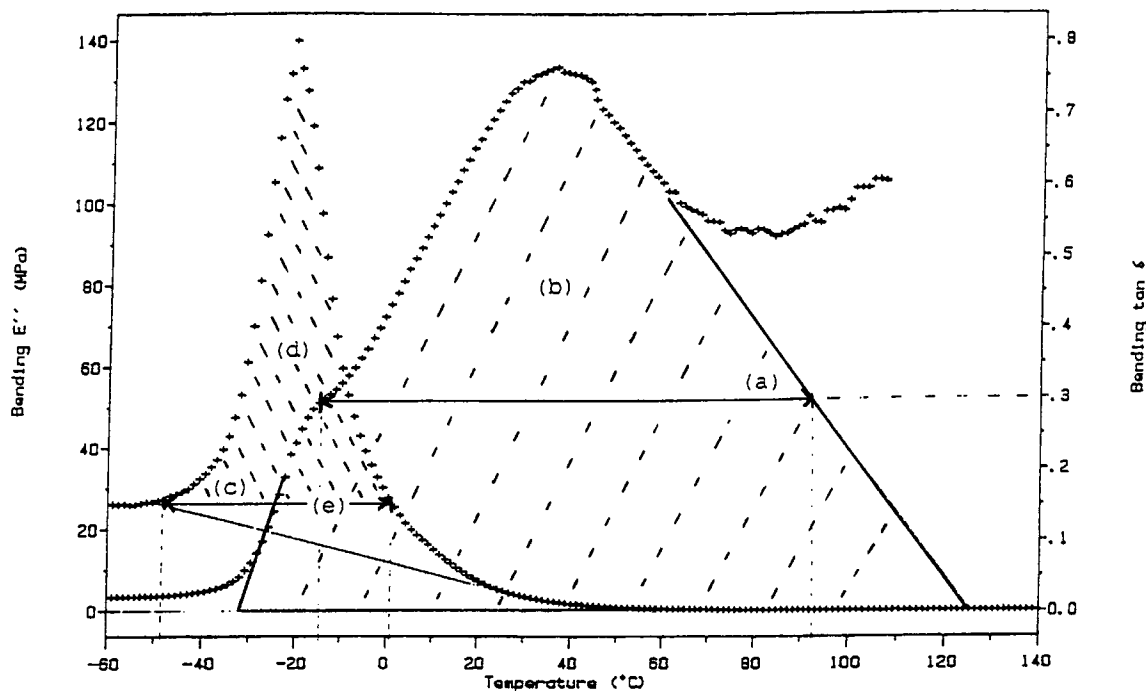


**Figure 6** DMTA data for the 70 : 30 linear PUR/PEMA blend. Illustration of (a) the loss factor temperature range where the  $\tan \delta$  values are greater than 0.3 ( $\tan \delta > 0.3$  [K]), (b) the extrapolation and area under the linear loss factor curve (TA [K]), (c) the loss modulus temperature range where the  $E''$  values are higher than at the constant value below  $T_g$  ( $E'' > E''_c$ ), (d) the area under the linear loss modulus curve above the constant  $E''$  (LA<sub>c</sub> [GPaK]) and (e) for the straight baseline type (LA [GPaK]).



The materials of both crosslinking studies were also investigated in terms of their damping characteristics. The areas under both the linear loss modulus curve, LA, and the linear loss factor curve, TA, have been used as an indication of the energy absorbing ability<sup>20,21</sup> of a material. Furthermore, the temperature range where the loss factor curves exhibits values of  $\tan \delta \geq 0.3$  are also commonly quoted.<sup>4,22</sup> In this study, LA is given with two different baseline corrections<sup>23</sup> and also the temperature range where the loss modulus is greater than the loss modulus value below  $T_g^9$  is indicated.

The calculation principles of the temperature range where  $\tan \delta \geq 0.3$ , TA, the temperature range where  $E'' > E''_c$  below  $T_g$  and both LA areas are shown in Figure 6 for the linear 70/30 PUR/PEMA polymer blend.

The loss factor data of the linear PUR/PEMA blend indicated that both polymers are semimiscible. The loss factor peak was higher than in any one of the IPNs. At 70°C, however, the material became too soft for measurement and material properties such as TA and the temperature range where  $\tan \delta \geq 0.3$  could only be approximated by extrapolation of the curve. The results for the damping characteristics of the 70 : 30 PUR/PEMA IPNs and both homopolymers are shown in Table III.

Looking at the loss factor, it may be noted that generally low crosslinking in the PUR network resulted in greater values for both the temperature range of  $\tan \delta > 0.3$  and TA. An exception to this was the IPN crosslinked at a diol/triol ratio of 3 : 1

and 5% TEGDM, which exhibited maxima for both the temperature range of  $\tan \delta > 0.3$  (130 K) and TA (62 K). 5% TEGDM crosslinking also proved to be the optimum level for the crosslinking of the PEMA network. Higher and lower crosslinking in the PEMA network resulted in lower values for both the temperature range of  $\tan \delta > 0.3$  and TA. Generally, the same tendency was observed for the temperature range of  $\tan \delta > 0.3$ , TA and also for the half-peak width (Table II).

The loss modulus versus temperature data revealed a different pattern, yet similar tendencies for both LA baseline types were observed. Both LAs seemed to increase slightly with higher crosslinking in the PUR, as did the temperature range where  $E'' > E''_c$ . On the other hand, both LAs and  $E'' > E''_c$  were not influenced to a significant extent by the crosslinking of the glassy network. This can be explained by the nature of  $E''$ . The latter is the product of the storage modulus and the loss factor. When a polymer undergoes  $T_g$ ,  $E'$  decreases by three to four decades, while  $\tan \delta$  values can, at best, increase by two decades from 0.02 to 2. Thus,  $E'$  determines  $E''$  to a large extent. In a broad IPN transition, the component at the higher temperature transition end does not make any contribution to  $E''$  because of the low  $E'$  value that overrides the  $\tan \delta$  increase. Generally, it has to be said that loss factor data showed excellent reproducibility, whereas the magnitude of the loss modulus data was much more susceptible to variations, which were due to variations in clamping the test specimen.

**Table III Damping Ability of the 70 : 30 PUR/PEMA IPN Composition as a Function of the Crosslink Density**

Crosslinking PUR/PEMA	Tan $\delta^a$ > 0.3 [K]	TA [K]	$E''^a > E''_c$	LA <sub>c</sub> [GPaK]	LA [GPaK]
1 : 1/5%	72	47.7	87	2.72	3.45
2 : 1/5%	79	50.6	58	2.42	3.14
3 : 1/10%	79	49.2	57	2.17	2.60
3 : 1/5%	130	62.1	58	2.21	2.68
3 : 1/2.5%	115	54.9	53	2.45	2.96
3 : 1/1%	96	54.4	49	2.12	2.65
3 : 1/0%	84	50.4	50	2.36	3.11
7 : 1/5%	125	59.0	45	2.57	3.02
1 : 0/5%	<sup>b</sup>	<sup>b</sup>	39	2.10	2.43
1 : 0/0%	(108) <sup>c</sup>	67.8	49	1.91	2.37
100 PUR (3 : 1) <sup>c</sup>	37	29.6	43	2.51	3.11
100 PEMA (5%) <sup>c</sup>	59	38.7	142	7.99	9.67

<sup>a</sup> The abbreviations are explained in Figure 1.

<sup>b</sup> Not available due to softening of the material.

<sup>c</sup> For values in brackets substantial curve extrapolation had to be conducted.

**Table IV Mechanical Properties of the 70 : 30 PUR/PEMA IPN as a Function of the Crosslink Density**

Crosslinking 70 : 30 IPN PUR/PEMA	Tensile Properties				Hardness Shore A
	Stress at Break (MPa)	Elongation at Break (%)	Young's Mod. (MPa)	Toughness (J)	
1 : 1/5%	13.3	280	33.5	7.9	92
2 : 1/5%	9.4	380	8.3	7.0	71
3 : 1/10%	9.6	380	8.0	7.5	77
3 : 1/5%	9.4	360	8.0	7.6	74
3 : 1/2.5%	8.5	450	7.6	7.0	71
3 : 1/1%	6.9	550	7.3	5.7	67
3 : 1/0%	6.7	640	6.2	6.8	61
7 : 1/5%	4.3	490	6.7	4.1	60
1 : 0/5%	0.8	200	2.5	0.3	45
1 : 0/0%	0.8	590	0.8	0.9	30
100 PUR (3 : 1)	1.2	210	1.0	0.6	40
100 PEMA (5%)	45	9.8	1300	0.9	99

The mechanical properties were investigated by tensile testing and hardness measurements. A compilation of the results is shown in Table IV.

In order to quantify the effect of the crosslinking on the mechanical properties, the stress at break and the strain at break were plotted against the  $M_{c,t}$  for both crosslink series. The steeper slope of the plot of the stress at break against  $M_{c,t}$  suggested that the crosslinking in the PUR network had a stronger effect on the IPN properties (Fig. 7).

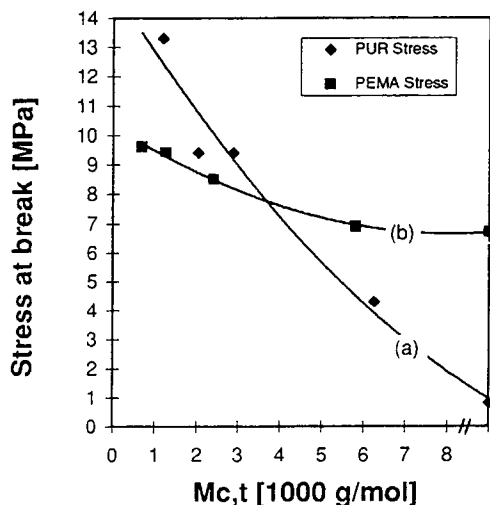


**Figure 7** Stress at break data versus the theoretical average molecular weight between crosslinks. The lines are the best fit through the (a) 70 : 30 PUR/PEMA (5% TEGDM) IPNs with different diol/triol ratios and (b) 70 : 30 PUR (D/T 3 : 1)/PEMA IPNs with different percentages of TEGDM.

The drop of the stress was more abrupt. However, a clear decrease in stress at break was also observed when decreasing the crosslink density of the PEMA. The strain at break versus  $M_{c,t}$  data showed very similar trends for both PUR and PEMA crosslinking (Fig. 8).

The only exception was the semi-2 IPN where the PUR was present in the linear form. This IPN

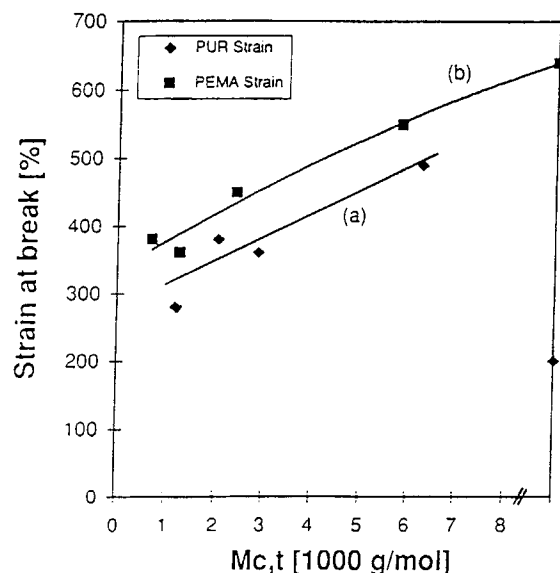


**Figure 8** Strain at break data versus the theoretical average molecular weight between crosslinks. The lines are the best fit through the (a) 70 : 30 PUR/PEMA (5% TEGDM) IPNs with different diol/triol ratios and (b) 70 : 30 PUR (D/T 3 : 1)/PEMA IPNs with different percentages of TEGDM.

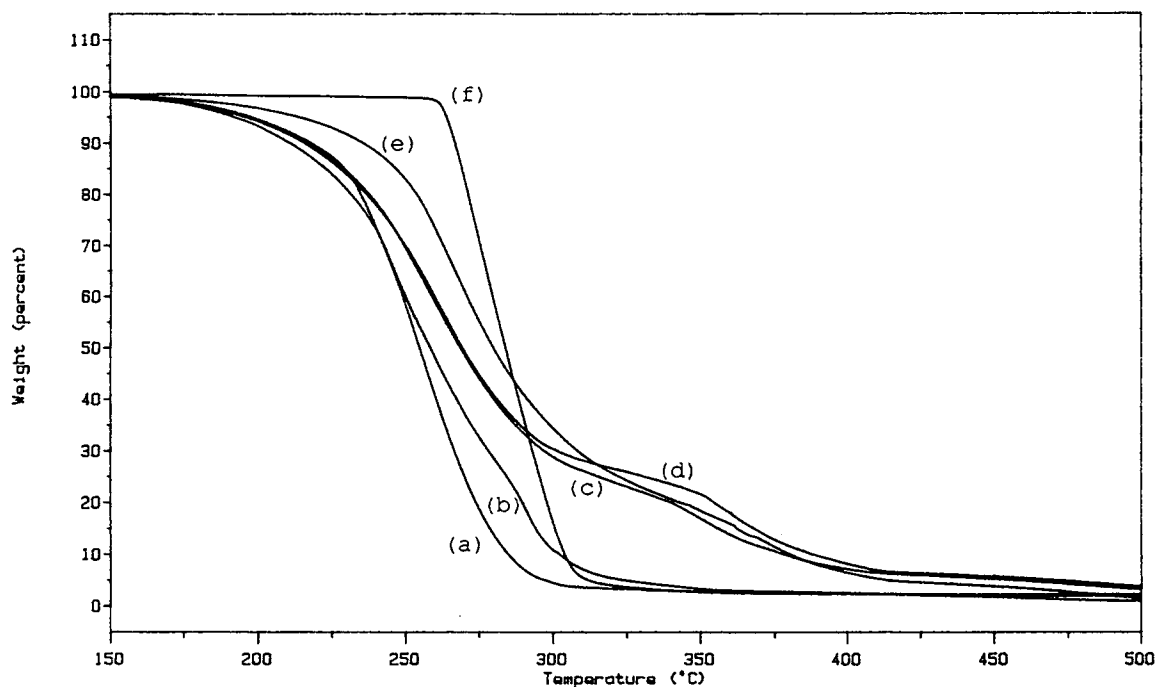


**Figure 9** Percent weight loss versus temperature. (a) the PUR (diol/triol 3 : 1) homonetwork, (b) the 70 : 30 PUR/PEMA linear blend, (c) the 70 : 30 PUR (3 : 1)/PEMA (5% TEGDM) IPN, (d) 70 : 30 PUR (3 : 1)/PEMA (10%), (e) 70 : 30 PUR (1 : 1)/PEMA (5%) and (f) the PEMA (5%) homonetwork.

resulted in the lowest strain at break (200%) of all materials. Generally, it was found that with lower crosslinking higher values for the strain at break were obtained. However, the change in the values were not as pronounced as for the ultimate stress data. As a consequence of the latter, higher values for the toughness index were obtained with the

higher crosslinked materials, which exhibited higher values for the stress at break. Higher crosslinking, especially in the PUR network, increased the Young's modulus from a value of 0.8 MPa for the 70 : 30 PUR/PEMA linear blend to 33.5 MPa for the respective IPN crosslinked at a diol/triol ratio of 1 : 1 and 5% TEGDM.

**Figure 10** TEM micrograph of the 70 : 30 PUR (diol/triol 3 : 1)/PEMA (5% TEGDM) IPN.

**Figure 11** TEM micrograph of the 70 : 30 PUR (diol/triol 1 : 1)/PEMA (5% TEGDM) IPN.

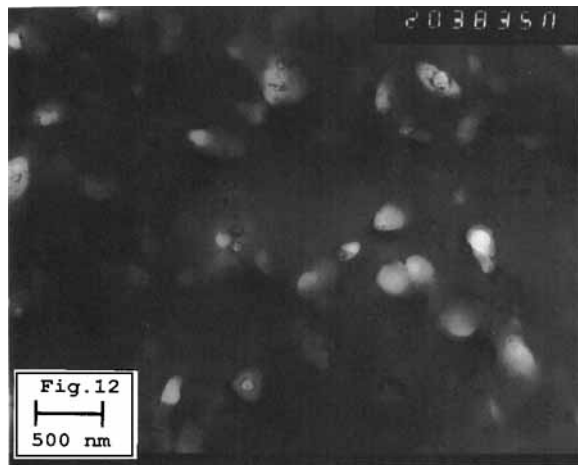


**Figure 12** TEM micrograph of the 70 : 30 PUR (diol/triol 3 : 1)/PEMA (10% TEGDM) IPN.

Thermogravimetric analysis was carried out on the two homopolymer networks, the 70 : 30 PUR/PEMA linear blend and IPNs of different crosslink density. The TGA traces revealed a different degradation pattern for the homopolymers and the respective IPNs (Fig. 9).

Both homopolymers degraded essentially in a one-step mechanism, whereas a two-step mechanism was observed for the IPNs. PEMA was thermally stable up to 270°C, whereas the PUR network started to decompose significantly at 200°C. Comparing four 70 : 30 PUR/PEMA compositions with different crosslinking degrees, considerable differences in the thermal stability were noted. The linear blend was clearly inferior to the IPNs. The three IPNs were crosslinked with a diol/triol ratio of 3 : 1 with 5% TEGDM, 3 : 1 with 10% TEGDM, and 1 : 1 with 5% TEGDM. It was noted that the crosslinking density in the PUR network determined the thermal properties of the IPNs. The IPN with the highest PUR crosslinking level was thermostable to the highest temperature. On the other hand, hardly any difference was noticed between the IPNs crosslinked with 5% and 10% TEGDM.

Transmission electron micrographs were prepared in order to investigate the influence of the crosslink density on the IPN morphology. The dark regions consist predominantly of polyurethane, which is preferentially stained by osmium tetroxide.<sup>24</sup> Three IPN samples were investigated by TEM. The broadest half-peak width, with 156°C (Table II), was obtained with the IPN crosslinked at a diol/triol ratio of 3 : 1 and 5% TEGDM. The TEM micrograph showed PEMA domains in the order of 100–300 nm (Fig. 10).

This material was compared with the IPN with the narrowest half peak width (72°C), which was crosslinked at a diol/triol ratio of 1 : 1 and 5% TEGDM. The TEM micrograph of this material showed a clearly finer phase structure (Fig. 11).

Besides the larger domain structure, also small domains between 50 and 100 nm were present. This confirmed earlier findings<sup>6</sup> that a tighter network of the material that forms first restricts the domain size of the second-formed network. Increasing the crosslink density of the second network was also investigated. Figure 12 shows the IPN crosslinked at a diol/triol ratio of 3 : 1 and with 10% TEGDM.

It can be seen that crosslinking in the second-formed PEMA network led to rather larger and better-defined phase domains. This confirmed the findings from the DMTA data of poorer phase mixing. With increasing crosslink density in the PEMA network, a coarser IPN was obtained. The higher crosslinked PEMA phase domains exhibited higher glass transition temperatures (Table II).

## CONCLUSIONS

It was shown that crosslinking could be used to adjust  $T_g$  location and the transition shape, and so tailor the damping peak. Crosslinking of the PUR network seemed to increase phase mixing, resulting in a narrower and higher transition shifted to higher temperatures. Crosslinking in the second-formed PEMA network decompatibilized the IPNs, which resulted in a broadening of the transition. The values for TA and the temperature range where  $\tan \delta > 0.3$  exhibited a maximum at diol/triol ratio of 3 : 1 and 5% TEGDM. However, generally, it was found that increased crosslinking decreased TA. LA values increased with higher crosslinking in the first formed (rubbery) network, yet levels in the second network did not have any influence at this 70 : 30 PUR/PEMA composition. Crosslinking of the PUR (first-formed network with higher weight percentage) exerted a stronger influence on the mechanical properties such as stress at break and Young's modulus. TGA results revealed a two-step degradation pattern for the IPNs, as opposed to the one-step pattern of both homopolymer networks. TEM micrographs confirmed that with higher crosslinking in the PUR smaller-phase domains resulted.

The authors would like to acknowledge John Bates at Loughborough University for preparing the TEM micrographs. One of the authors (F.-U.S.) would like to ac-

knowledge a grant from the German Academic Exchange Service, DAAD.

## REFERENCES

1. D. Klemptner and L. Berkowski, in *Encyclopedia of Polymer Science and Engineering*, H. Mark, N. M. Bikales, C. G. Overberger, and G. Menges, eds., Vol. 8, Wiley, New York, 1988.
2. L. H. Sperling, in *Interpenetrating Polymer Networks*, ACS 239, D. Klemptner, L. H. Sperling, and L. A. Utracki, eds., ACS, Washington, DC, 1994.
3. L. H. Sperling, *Interpenetrating Polymer Networks and Related Materials*, Plenum Press, New York, 1981.
4. D. J. Hourston and F.-U. Schäfer, *Polym. Adv. Technol.*, to appear.
5. A. A. Donatelli, L. H. Sperling, and D. A. Thomas, *J. Appl. Polym. Sci.*, **21**, 1189 (1977).
6. A. A. Donatelli, L. H. Sperling, and D. A. Thomas, *Macromolecules*, **9**, 671, 676 (1976).
7. Q. Chen, H. Ge, D. Chen, X. He, and X. Yu, *J. Appl. Polym. Sci.*, **54**, 1191 (1994).
8. D. J. Hourston and F.-U. Schäfer, *Polymer*, accepted.
9. D. J. Hourston and F.-U. Schäfer, *High Perform. Polym.*, **8**, 1 (1996).
10. M. Tagayuki, *Dynamic mechanical properties of polymeric materials*, Elsevier, Amsterdam, 1978.
11. G. Tieghi, M. Levi, A. Fallini, and F. Danusso, *Polymer*, **32**, 39 (1991).
12. V. E. Shashoua and R. G. Beaman, *J. Polym. Sci.*, **33**, 101 (1958).
13. L. E. Nielsen, *Mechanical Properties of Polymers*, Reinhold, New York (1967).
14. P. J. Flory and J. Rehner, *J. Chem. Phys.*, **11**, 521 (1943).
15. J. P. Bell, *J. Polym. Sci.*, A2, **8**, 417 (1970).
16. G. M. Bristow and W. F. Watson, *Trans. Faraday Soc.*, **54**, 1731 (1958).
17. V. Mishra, F. Du Prez, and L. H. Sperling, *Polym. Mater. Sci. Eng.*, **72**, 124 (1995).
18. M. T. Tabka, J.-M. Widmaier, and G. C. Meyer, *Plastics Rubber Comp. Process. Appl.*, **16**, 11 (1991).
19. R. B. Fox, J. L. Bittner, J. A. Hinkley, and W. Carter, *Polym. Eng. Sci.*, **25**, 3, 157 (1985).
20. M. C. O. Chang, D. A. Thomas, and L. H. Sperling, *J. Appl. Polym. Sci.*, *Polym. Phys.*, **26**, 1627 (1988).
21. M. C. O. Chang, D. A. Thomas, and L. H. Sperling, *J. Polym. Mater.*, **6**, 61 (1989).
22. S. Yao, M. Jia, X. Yan, and Y. Wang, in *Polymers and Biomaterials*, H. Feng, Y. Han, and L. Huang, eds., Elsevier B. V. (1991).
23. J. Fay, D. A. Thomas, and L. H. Sperling, *J. Appl. Polym. Sci.*, **43**, 1617 (1991).
24. K. Kato, *Polym. Eng. Sci.*, **1**, 38 (1967).

Received March 4, 1996

Accepted June 27, 1996